Am J Cancer Res 2023;13(9):4418-4433
www.ajcr.us /ISSN:2156-6976/ajcr0152971

Original Article

Construction and experimental validation of a necroptosis-related lncRNA signature as a prognostic model and immune-landscape predictor for lung adenocarcinoma

Tongtong Zhang[2*], Ruoxuan Hei[3*], Yue Huang[1*], Jingjin Shao[1], Min Zhang[1], Kai Feng[2], Weishen Qian[2], Simin Li[3], Faguang Jin[2], Yanwei Chen[1,2]

[1]Department of Pulmonary Critical Care Medicine, The 1st Affiliated Hospital of Shenzhen University, Shenzhen 518035, Guangdong, PR China; [2]Department of Pulmonary Critical Care Medicine, The Second Affiliated Hospital of The Air Force Military Medical University, Xinsi Road 569, Xi'an 710038, Shaanxi, PR China; [3]Department of Clinical Diagnose, The Second Affiliated Hospital of The Air Force Military Medical University, Xinsi Road 569, Xi'an 710038, Shaanxi, PR China. [*]Co-first authors.

Received August 16, 2023; Accepted September 14, 2023; Epub September 15, 2023; Published September 30, 2023

Abstract: Necroptosis is a new form of cell death. Since the discovery that long non-coding RNAs can affect the proliferation of lung adenocarcinoma, much has been learned about it, yet those of necroptosis-related long non-coding RNAs (NRIncRNAs) in lung adenocarcinoma (LUAD) remain enigmatic. This study aims to explore novel biomarkers and therapeutic targets for LUAD. The LUAD data was downloaded from The Cancer Genome Atlas, and necroptosis-related genes were retrieved from published literature. Co-expression analysis, univariate Cox analysis, least absolute shrinkage and selection operator regression analysis were used to identify necroptosis-related prognostic long non-coding RNAs. A comprehensive evaluation of tumor immunity for necrosis-related features was performed, and we identified a 9-NRIncRNA signature. Kaplan-Meier and Cox regression analyses confirmed that the signature was an independent predictor of LUAD outcome in the test and train sets (all $P < 0.05$). The areas of 1-, 2-, and 3-year overall survival under the time-dependent receiver operating characteristics (ROC) curve (AUC) were 0.754, 0.746, and 0.720, respectively. The GSEA results showed that 9 NRIncRNAs were associated with multiple malignancy-associated and immunoregulatory pathways. Based on this model, we found that the immune status and level of response to chemotherapy and targeted therapy were significantly different in the low-risk group compared with the high-risk group. qRT-PCR assay revealed that 9 NRIncRNAs were involved in the regulation of tumor cell proliferation and may affect the expression of programmed cell death 1 (PD1) and CD28 at human immune checkpoints. Our results indicated that the novel signature involving 9 NRIncRNAs (*AL031600.2, LINC01281, AP001178.1, AL157823.2, LINC01290, MED4-AS1, AC026355.2, AL606489.1, FAM83A-AS1*) can predict the prognosis of LUAD and are associated with the immune response. This will provide new insights into the pathogenesis and development of therapies for LUAD.

Keywords: Lung adenocarcinoma, gene signature, necroptosis, immunity

Introduction

Lung cancer is the leading cause of cancer-related deaths worldwide [1], in which lung adenocarcinoma (LUAD) is the most common historical type [2]. Although precise treatment strategies including immunotherapy and molecularly targeted therapies such as anti-PD-1/PD-L1 immune checkpoint inhibitors (ICIs) have significantly improved outcomes, most advanced non-small cell lung cancer (NSCLC) developed chemotherapy resistance and progressed [3]. The 5-year survival rates for LUAD were only 15% [4]. Therefore, it is vital to identify exploitable diagnostic biomarkers and therapeutic targets.

Apoptosis resistance is a major cause of chemotherapy failure [5]. Necroptosis, served as an alternative type of regulated cell death, has

been well-established to overcome the obstacle. The core mediators of the necroptotic pathway conclude Receptor-Interacting Protein 1 (RIP1), RIP3, and Mixed Lineage Kinase Domain-Like (MLKL) [6]. On the one hand, accumulating evidence indicate that necroptosis played pivotal roles in tumorigenesis, cancer progression, cancer metastasis [7-9]; on the other hand, it may activate cytotoxic CD8+ T lymphocytes, leading to tumor cells elimination [10]. In addition, necroptosis has also been demonstrated to induce an immune suppressive tumor microenvironment (TME) [11]. Considering the critical role of necrosis in cancer biology, necroptosis may trigger antitumor immunity in cancer therapy and become a new target for cancer therapy [6, 12].

Long non-coding RNAs (lncRNAs) are defined as ncRNAs of at least 200 nucleotides (nt) in length that molecularly resemble mRNA [13]. Previous studies indicated that lncRNAs exert important regulatory functions on gene expression at the transcriptional, post-transcriptional, and epigenetic levels [14]. Abnormally expressed lncRNAs can effect multiple cellular and physiologic functions of cells, such as cell cycle, migration, invasion, proliferation, multidrug resistance [15, 16]. Recently, lncRNAs as emerging cancer biomarkers have been used in the diagnosis and prediction of survival in multiple cancer types. For example, LncRNA XLOC_009167 was overexpressed in lung cancer tissues and showed a better diagnostic potential [17, 18]. The study of NRlncRNAs has not been widely mentioned as a potential therapeutic target in LUAD. Therefore, acquiring more NRlncRNAs knowledge can help us understand the roles of necroptosis and lncRNAs in immunotherapy clearly.

With the development of high-throughput sequence technology, bioinformatics has become increasingly popular in genomic analysis to investigate the pathological mechanism of the tumor and discover tumor-specific biomarkers. In recent years, gene signatures have been widely studied, such as colon cancer, breast cancer, and hepatocellular carcinoma [18-20], which are helpful for the selection of lung cancer treatment methods and the prediction of survival probability after lung cancer surgery. In the present study, we utilized least absolute shrinkage and selection operator regression analysis (LASSO) regression analysis, univariate and multivariate Cox regression analyses, survival analysis to identify lncRNAs related to the prognosis of LUAD on the basis of diverse bioinformatic methods. We constructed and verified a 9-NRlncRNA signature for forecasting the prognosis and immune response of LUAD. Finally, the effects of 9 NRlncRNAs on cell proliferation levels in lung adenocarcinoma cells were examined. And in order to verify whether they have an effect on PD1/CD28, PCR experiments were performed. Our findings should help to improve the early diagnosis rate of LUAD and provide a theoretical basis for precise, individualized treatment.

Materials and methods

Acquisition and preprocess data

The transcriptome profiling (HTSeq- FPKM format) and clinical information of LUAD and normal samples were downloaded from the Cancer Genome Atlas database (TCGA, https://portal.gdc.cancer.gov/). The Practical Extraction and Report Language (Perl) software was exploited to merge the age, gender, survival time, survival status, tumor stage and TNM stage of patients with LUAD into a single file. The gene transfer format (GTF) files were obtained from Ensembl database (http://asia.ensembl.org) to distinguish mRNAs and lncRNAs. Subsequently, a cohort of 67 necroptosis-related genes (NRGs) were abstracted from the previous literatures [21]. We identified NRlncRNAs by Pearson correlation analysis between NRGs and lncRNAs with criteria of coefficients > 0.40 and $P < 0.05$. In order to explore the regulatory mechanism, the co-expression network of NRGs and lncRNAs was built by igraph R package. The limma R package was used to screen differentially expressed NRlncRNAs (DENRlncRNAs) between LUAD samples and normal samples ($|Log2FC| > 1.5$ and $P < 0.05$) for further study. Sankey diagram was plotted by ggalluvial and ggplot2 R package.

Construction and validation of risk model

Univariate Cox regression analysis was applied to screen the NRlncRNAs of which expression levels were significantly correlated with overall survival (OS) time of patients with LUAD ($P < 0.05$), and 20 prognostic NRlncRNAs were identified. They were subsequently incorporat-

ed into a Cox proportional hazard regression analysis, and a heatmap was plotted by pheatmap R package for visualization. The LASSO regression was then utilized to narrow down the candidate NRlncRNAs. Ultimately, 9 NRlncRNAs and their coeffcients were retained to establish the prognostic model by glmnet R package. We calculated the risk score with the following formula:

$$risk\ score = \sum_{i}^{9} Xi \times Yi$$

(*X*: coefficients, *Y*: lncRNA expression level)

According to the median value of risk score, the TCGA LUAD patients were divided into low- and high-risk subgroups. The "survival", "survminer" and "pheatmap" R package were utilized to perform the survival analysis and compare the survival probability, distribution of risk score, survival status and survival probability between the two groups in train, test and all sets, respectively.

Independent prognostic factors and ROC

Univariate and multivariate Cox regression analyses were carried out to identify weather the risk score and clinicopathological factors were independent prognostic factors. The "survival", "survminer" and "timeROC" R package were used to plot the 1-, 2- and 3-year Receiver operating characteristics (ROC) curves of the prognostic model, and different ROC curves to compare variable factors in predicting survival probability. The nomogram was developed using the rms R package.

Gene set enrichment analysis

With curated gene set (kegg.v7.4.symbols.gmt), gene set enrichment analyses (GSEA) software (https://www.gsea-msigdb.org/gsea/login.jsp) was applied to identify the significantly enriched pathways between the low- and high-risk groups based on the criterion: $P < 0.05$ and FDR < 0.25.

Investigation of the TME and immune checkpoints

According to the result of GSEA, we decided to analyze the immune-cell factors in risk groups. We could calculate the immune infiltration statuses among the LUAD patients from the TCGA including TIMER, CIBERSORT, XCELL, QUANTISEQ, MCPcounter, EPIC, and CIBERSORT on TIMER2.0 (http://timer.cistrome.org/). In another way, we could download the profile of infiltration estimation for all TCGA tumors on the same website. Wilcoxon signed-rank test, limma, scales, ggplot2, and ggtext R packages were performed in analyzing the differences in immune infiltrating cell content explored. Besides, we also made comparisons about TME scores and immune checkpoints activation between low- and high-risk groups by ggpubr R package.

Exploration of the model in the clinical treatment

Then we used the R package pRRophetic to evaluate their therapy response determined by the half-maximal inhibitory concentration (IC50) of each LUAD patient on Genomics of Drug Sensitivity in Cancer (GDSC) (https://www.cancerrxgene.org/).

Cell line and culture

The lung adenocarcinoma cell line A549 was obtained from Shanghai Cell Collection (Shanghai, China). A549 cells were maintained in Ham's F-12K (Kaighn's) with 10% fetal bovine serum (FBS; Gibco, Gaithersburg, MD, USA) and cultured 37°C in 5% CO_2.

RNA extraction and qRT-PCR

Total RNA was isolated from A549 cells using TRIzol reagent (Invitrogen, Carlsbad, CA, USA) according to the manufacturer's instructions. The PrimerScript regent Kit (TAKARA, Dalian, China) were used to reverse-transcribe purified RNA samples. Quantitative gene expression by qRT-PCR was performed using the Blastaq™ 2× qPCR MasterMix (abm, Canada) according to the instructions. The relative levels of lncRNAs expression were normalized to the GAPDH level. The relative expression level of each gene was calculated by the $2^{-\Delta\Delta Ct}$ method. All primer sequences are shown in Table S3.

Cell transfection

The siRNAs and negative control (NC) were designed by Tsingke Biotech Co., (Beijing, China). Prior to cell transfection, the cells were inoculated in a 6-well plate until the cell density reached approximately 60%, and then siRNA

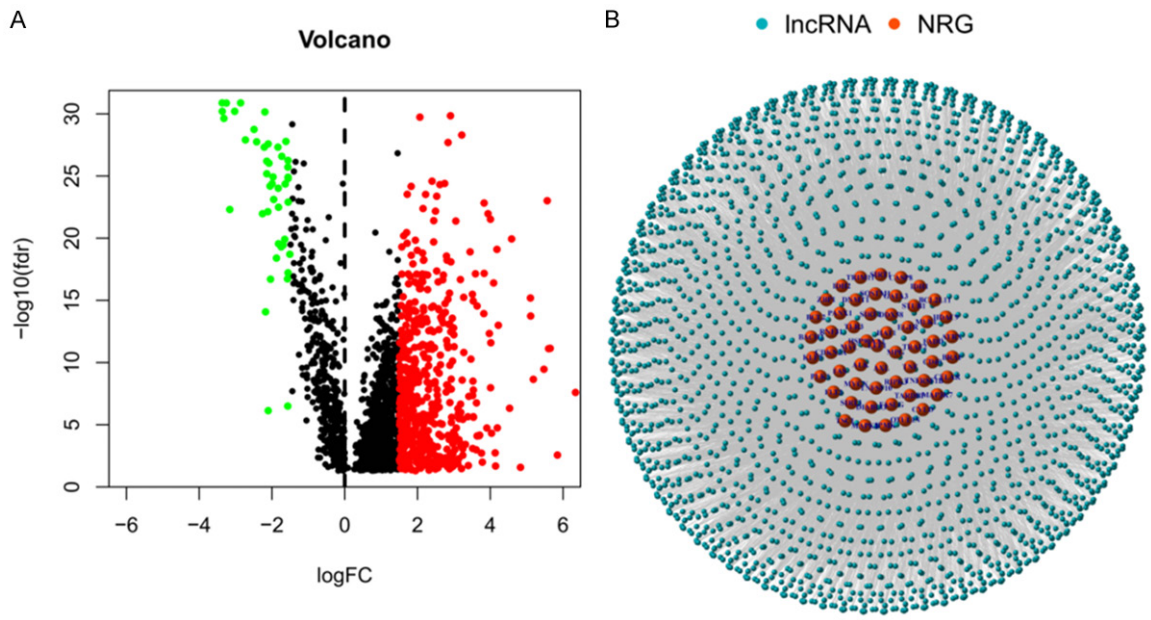

Figure 1. Expression of 576 differential expressed NRlncRNAs and the interaction between them and NRGs in patients with LUAD. A. The volcano plot of the NRlncRNAs between the tumor and normal tissues (red: up-regulated NRlncRNAs; green: down-regulated NRlncRNAs); B. The network between NRGs and lncRNAs (correlation coefficients > 0.4 and $P < 0.001$).

was transfected using the X-tremeGENE siRNA transfection reagent (Roche) according to the manufacturer's instructions. The transfection efficiency of siRNA was verified by qRT-PCR.

Colony formation assay

Transfected A549 cells were inoculated at the density of 500 cells per well, cultured for 15 days. At the end of the experiment, the cells were washed twice with pre-cooled phosphate buffered saline (PBS), fixed with 1 ml of 4% paraformaldehyde for 30 minutes, and then stained with 1% crystal violet for 30 minutes. Cell colony forming ability was determined by counting cell clones of 50 or more cells.

Statistical analysis

All computational and statistical analyses were conducted using R (version4.0.3). Survival analysis was performed using the Kaplan-Meier method. The Kruskal-Wallis test was used to compare differences between groups. The chi-squared test or Fisher's exact test was used for analyses of clinical information. Spearman or Pearson correlation coefficients were used to evaluate the relationships among lncRNA expression, immune infiltration, and immune checkpoint gene expression. The difference between the two groups was compared using the Student's *t*-test, while the one-way analysis of variance (ANOVA) test was performed for statistical analysis of three groups or more.

Result

Identification of NRlncRNAs

From TCGA database, a total of 594 transcription data and the corresponding clinical information (535 LUAD samples and 59 normal samples) were downloaded. Patients survived < 30 days were excluded. First, we identified 67 NRGs (Table S1). Then, 2154 NRlncRNAs were screened based on Pearson correlation analysis. The necroptosis-related lncRNA-mRNA co-expression network and data were shown in **Figure 1B**. Subsequently, we filtered out 576 differentially expressed NRlncRNAs between tumor samples and normal samples, and among them, 531 were enriched in the LUAD samples while 45 were downregulated. The volcano was showed in **Figure 1A**. We finally retrieved 490 patients and randomly divided them into the train risk group and test risk group by Strawberry Perl and caret R package. The ratio was 1:1.

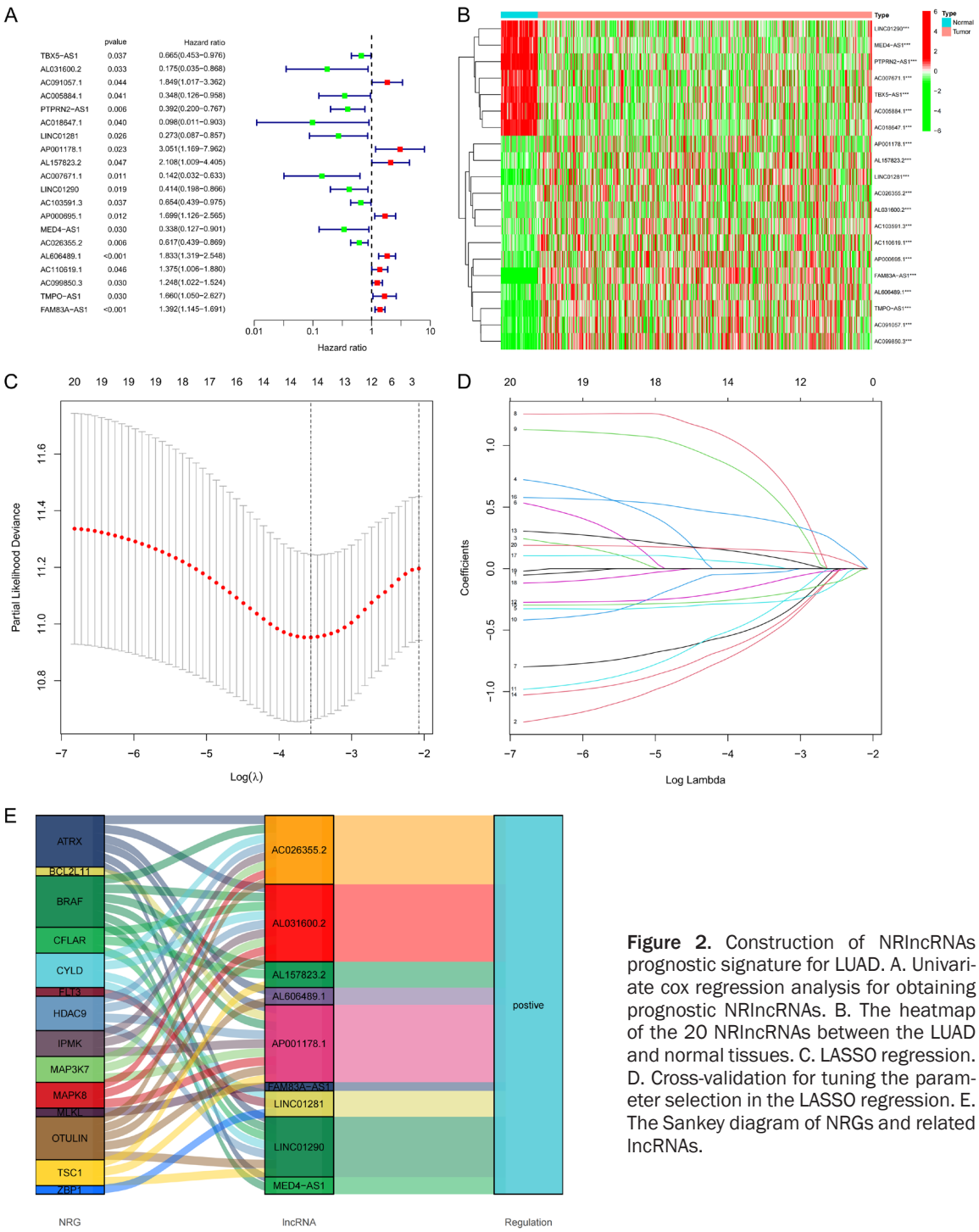

Figure 2. Construction of NRIncRNAs prognostic signature for LUAD. A. Univariate cox regression analysis for obtaining prognostic NRIncRNAs. B. The heatmap of the 20 NRIncRNAs between the LUAD and normal tissues. C. LASSO regression. D. Cross-validation for tuning the parameter selection in the LASSO regression. E. The Sankey diagram of NRGs and related lncRNAs.

Construction and verification of a prognostic gene risk model

A cohort of 490 LUAD samples corresponding with patients had complete survival information. The 20 NRIncRNAs (TBX5-AS1, AL031600.2, AC091057.1, AC005884.1, PTPRN2-AS1, AC018647.1, LINC01281, AP001178.1, AL157823.2, AC007671.1, LINC01290, AC103591.3, AP000695.1, MED4-AS1, AC026355.2, AL606489.1, AC110619.1, AC099850.3, TMPO-AS1, FAM83A-AS1) were preliminarily screened by univariate cox regression analysis for further analysis, indicating these genes were associated with patients' OS (**Figure 2A**, **2B** and Table S2). Moreover, in

order to avoid overfitting the signature, we utilized LASSO Cox regression analysis and finally obtained 9 NRlncRNAs (AL031600.2, LINC01281, AP001178.1, AL157823.2, LINC01290, MED4-AS1, AC026355.2, AL606489.1, FAM83A-AS1) to construct the risk signature (**Figure 2C**, **2D**), and among them, 5 lncRNAs (AL031600.2, LINC01281, LINC01290, MED4-AS1, AC026355.2) were protective genes with HR < 1, while the other 4 lncRNAs (AP001178.1, AL157823.2, AL606489.1, FAM83A-AS1) with HR > 1 were correlated with increased risk. In addition, we could find all of the 9 NRlncRNAs were positively associated with NRGs in the Sankey diagram (**Figure 2E**).

The risk score for each LUAD patients was calculated as follows: risk score = (-1.322* *AL031600.2* exp.) + (-1.043* *LINC01281* exp.) + (1.539* *AP001178.1* exp.) + (1.007* *AL157823.2* exp.) + (-0.715* *LINC01290* exp.) + (-1.089* *MED4-AS1* exp.) + (-0.297* *AC026355.2* exp.) + (0.570* *AL606489.1* exp.) + (0.223* *FAM83A-AS1* exp.). According to the median value of risk score, 490 LUAD patients were separated into high- and low-risk group. We then compared the distribution of risk score, survival status and survival probability between the high- and low-risk group in train, test and all sets, respectively. Patients in the low-risk group had a longer survival time and less deaths than that in the high-risk group. Significant difference could be observed between the high- and low-risk groups (**Figure 3A-L**).

Independent prognostic value of the risk model and clinicopathological factors

We used univariate and multivariable Cox regression analyses to evaluate whether the risk score derived from the 9-NRlncRNA signature model could serve as an independent prognostic factor (**Figure 4** and **Table 1**). The univariate Cox regression analysis indicated that the risk score was an independent factor predicting poor survival (HR=1.146, 95% CI: 1.101-1.193, **Figure 4A**). The multivariate analysis also implied that, after adjusting for other confounding factors, the risk score was a prognostic factor (HR=1.157, 95% CI: 1.108-1.207, **Figure 4B**) for patients with LUAD. We also found stage could be an independent prognostic factor ($P < 0.001$, **Figure 4A**, **4B**). Time-dependent ROC analysis was carried out to evaluate the sensitivity and specificity of the prognostic model, and we found that AUC was 0.754 for 1-year, 0.746 for 2-year, and 0.720 for 3-year survival (**Figure 4C**), which was better than any other parameters (**Figure 4D**). According to two independent prognostic factors, risk score and tumor stage (all $P < 0.001$ in multivariable Cox regression), we built a nomogram for predicting the 1-, 3-, and 5-year OS incidences of LUAD patients (**Figure 4E**). We also utilized the 1-, 3-, and 5-year OS calibration plots to attest that the nomogram had a good concordance with the prediction of 1-, 3-, and 5-year OS (**Figure 4F**). Furthermore, clinicopathological parameters including age, gender, tumor stage, T, N, and M were compared between the high- and low-risk group (Figure S1).

GSEA

GSEA was performed for functional annotation. The top 10 KEGG pathways are shown in **Figure 5.** Cell cycle (NES=2.30, P=0.000), small cell lung cancer (NES=2.14, P=0.000), p53 signaling pathway (NES=2.03, P=0.000), base excision repair (NES=2.09, P=0.000), gap junction (NES=2.02, P=0.000), pyrimidine metabolism (NES=2.00, P=0.000), pathways in cancer (NES=1.91, P=0.000), DNA replication (NES=1.87, P=0.000), ECM receptor interaction (NES=1.80, P=0.028) and Notch signaling pathway (NES=1.77, P=0.016) were all enriched in high-risk group. The results indicated that the lncRNAs of the new signature maybe associated with tumorigenesis. There were also immune-related pathways, such as Notch signaling pathway. Thus, we further explored the link between the signature and immune.

Relationship between risk score and immune cell infiltration and differences in the response to immunotherapy chemotherapy, and targeted therapy between high-risk and low-risk groups

Subsequently, the relationship between immune cell infiltration and risk score was performed by R software. In our results (**Figure 6**), risk score was significantly positively correlated with CD4+ Th1 cells (R=0.13, P=0.0046)

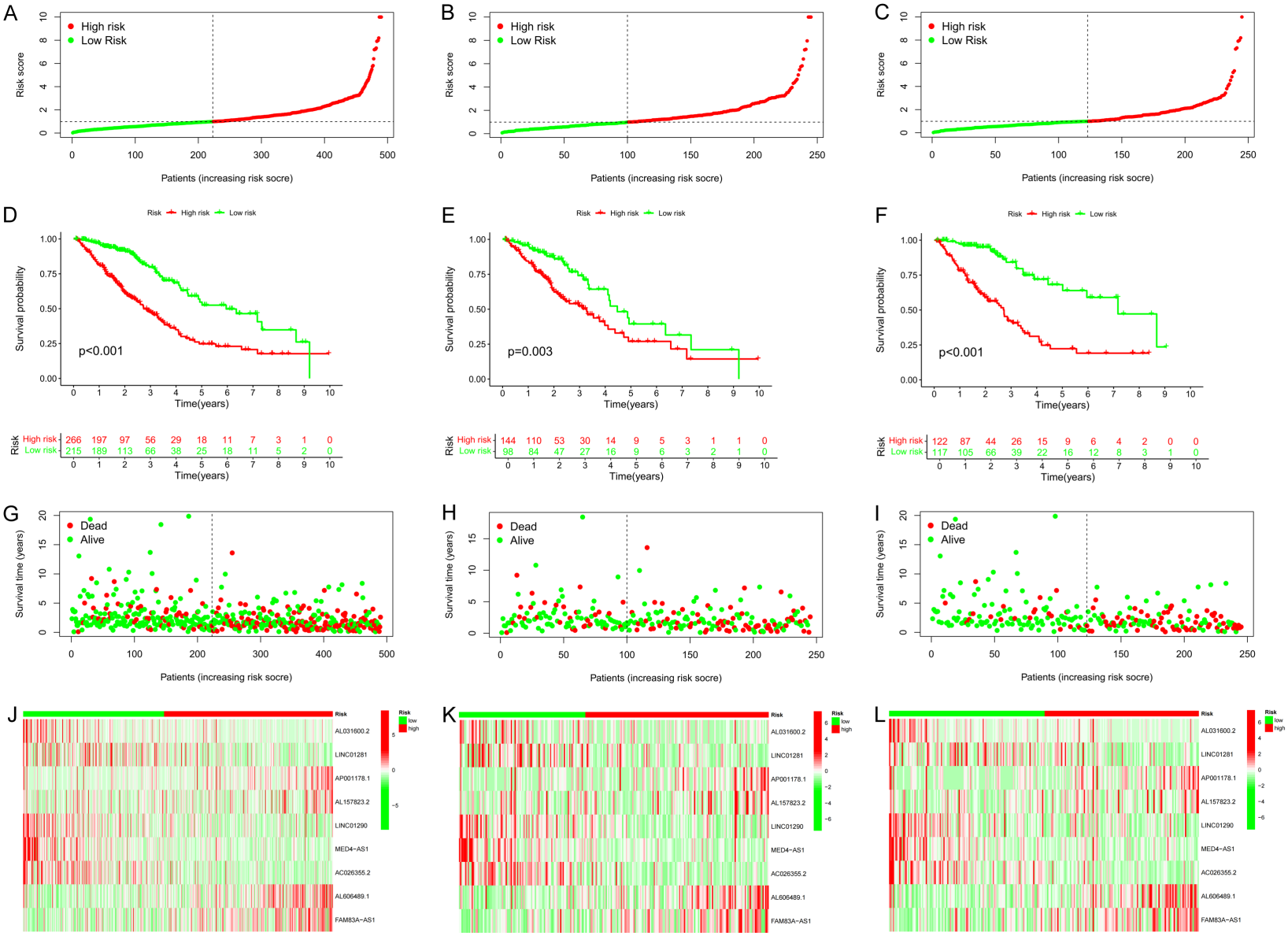

Figure 3. Prognosis value of the 9-NRIncRNA model in the entire, test and train sets. A-C. Survival status between low- and high-risk groups in the entire, test and train sets, respectively. D-F. Kaplan-Meier survival curves of OS (survival probability) of patients between low- and high-risk groups in the entire, test and train sets, respectively. G-I. Survival time between low- and high-risk groups in the entire, test and train sets, respectively. J-L. The heat map of 9 NRIncRNAs expression in the in the entire, test and train sets, respectively.

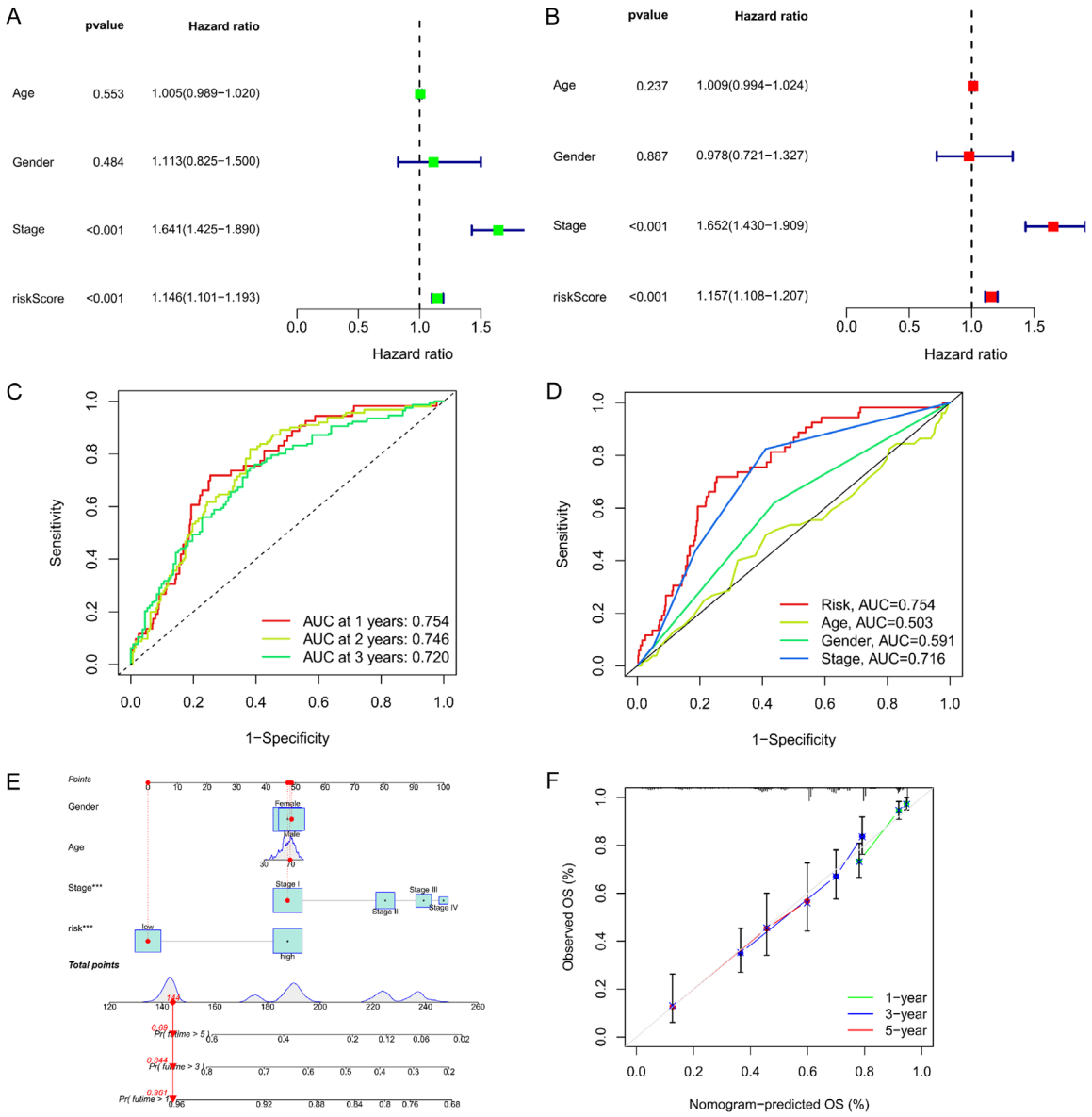

Figure 4. Univariate and multivariate Cox regression analyses for the risk score. A. Univariate analysis for the TCGA cohort. B. Multivariate analysis for the TCGA cohort. C. The calibration curves for 1-, 2-, and 3-year ROC curves. D. The 3-year ROC curves of risk score, and clinical characteristics. E. The nomogram that integrated the risk score, age, and tumor stage predicted the probability of the 1-, 3-, and 5-year OS. F. The calibration curves for 1-, 3-, and 5-year OS.

and CD4+ Th2 cells (R=0.27, *P*=8.5e-10), and it was significantly negative correlated with B cell (R=-0.21, *P*=1.9e-06), cancer associated fibroblast (R=-0.3, *P*=9.6e-12), macrophage (R=-0.19, *P*=2.8e-05), mast cell (R=-0.16, *P*=0.00026), monocyte (R=-0.12, *P*=0.0063), myeloid dendritic cell (R=-0.34, *P*=1.9e-14), CD8+ T cells (R=-0.22, *P*=5e-07), NK cell (R=-0.12, *P*=0.0058), Treg cell (R=-0.24, *P*=7.8e-08) and endothelial cell (R=-0.14, *P*=0.0021). Based on the functional analyses, we compared the enrichment scores of 16 types of immune cells and the activity of 13 immune-related pathways between the low- and high-risk groups by employing the single-sample gene set enrichment analysis (ssGSEA). The low-risk subgroup generally had higher levels of infiltration of immune cells, especially of dendritic cells, B cells, mast cells, neutrophils, T helper cells, and TIL than the high-risk

Table 1. Univariate and multivariate analyses for overall survival in patients with LUAD obtained from TCGA

Variables	Univariate analysis			Multivariate analysis		
	HR	95% CI	*P* value	HR	95% CI	*P* value
Age	1.005	0.989-1.020	0.553	1.009	0.994-1.024	0.237
Gender	1.113	0.825-1.500	0.484	0.978	0.721-1.327	0.887
Stage	1.641	1.425-1.890	5.73-12*	1.652	1.430-1.909	9.40-12*
riskScore	1.146	1.101-1.193	1.78-11*	1.157	1.108-1.207	2.40-11*

HR: hazard ratio, 95% CI: 95% confidence interval; *, statistically significant.

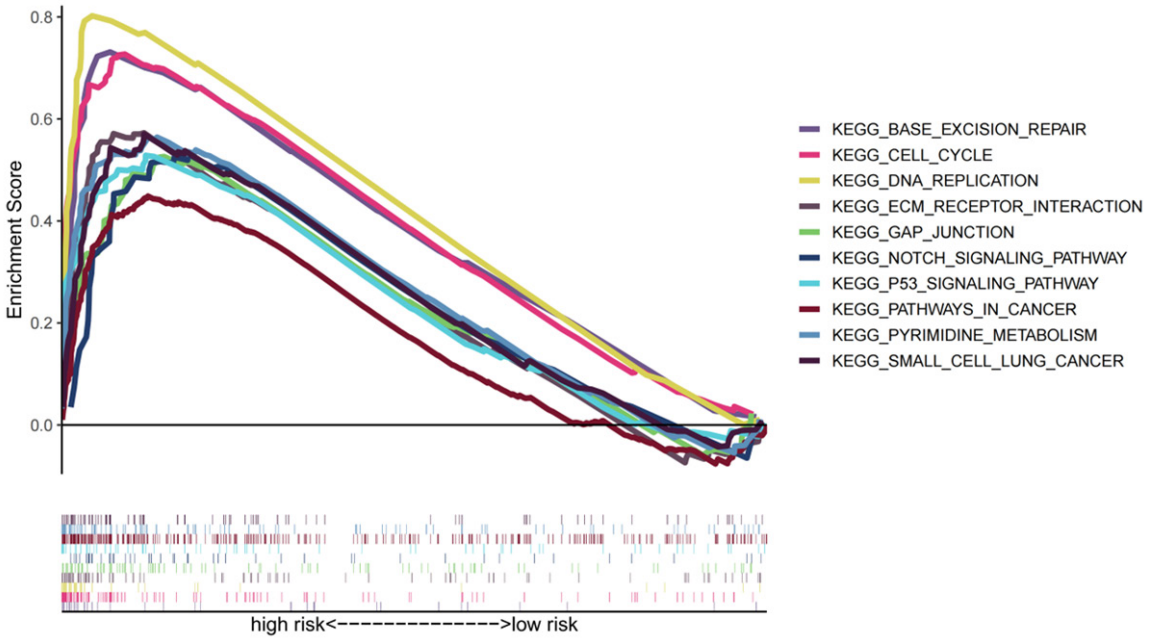

Figure 5. The top 10 pathways significantly enriched in the high-risk group by GESA, including cell cycle, small cell lung cancer, p53 signaling pathway, base excision repair, gap junction, pyrimidine metabolism, pathways in cancer, DNA replication, ECM receptor interaction and Notch signaling pathway.

subgroup. Four immune pathways, including Human Leukocyte Antigen (HLA), major histocompatibility complex I (MHC I), T cell co-stimulation and Type2 interferon (IFN) response showed lower activity in the high-risk group than in the low-risk group (Figure S2A, S2B). The low-risk group had higher immune score, stromal score and estimates score (Figure S2C-E). All of those showed low-risk group had higher immune infiltration status. Based on these findings, the poor survival outcome of high-risk LUADs may be caused by decreased levels of antitumour immunity.

The expression levels of immune checkpoints and/or their ligands may constitute predictive biomarkers for immune checkpoint blockade therapy. We further investigated the relationship between the levels of 22 ICI genes and the two risk groups. Low-risk patients tended to express higher levels of 20 immune checkpoint genes, including CTLA4, CD40LG, VSIR, CD160, TNFRSF25, TNFRSF14, HAVCR2, IDO2, TNFSF15, CD80, ICOS, CD28, TIGIT, CD86, CD200R1, CD244, and BTLA, while CD276 was highly expressed in high-risk patients (Figure S3A, $P < 0.05$). It implied that we could choose appropriate checkpoint inhibitors for LUAD patients regrouped by the risk model.

In addition, we assessed the relation between the risk score and the efficacy of chemotherapeutics and targeted therapeutics for LUAD. Patients with low-risk scores were highly sensi-

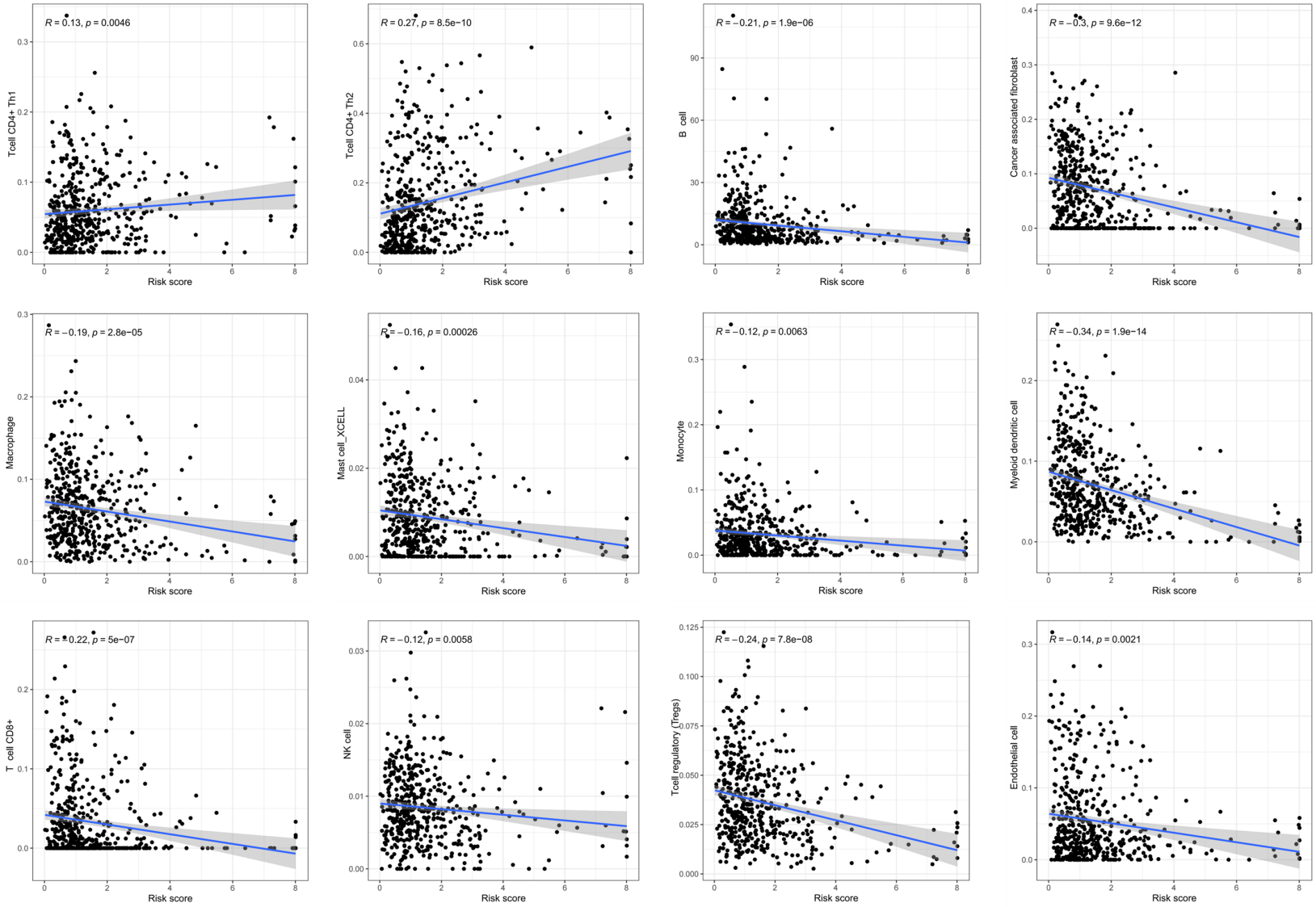

Figure 6. The correlation between risk score and immune cells. Risk score was significantly positively correlated with CD4+ Th1 cells and CD4+ Th2 cells, and it was significantly negative correlated with B cell, cancer associated fibroblast, macrophage, mast cell, monocyte, myeloid dendritic cell, CD8+ T cells, NK cell, Treg cell and endothelial cell.

tive to the targeted therapeutics gefitinib (*P*=0.0025) and erlotinib (*P*=1.5e-07). In addition, patients with low-risk scores were highly sensitive to the chemotherapeutics etoposide (*P*=0.0037), paclitaxel (*P*=5.7e-07), docetaxel (*P*=3.8e-08) and Gemcitabine (*P*=0.034), suggesting that the risk signature is a potential predictor of chemosensitivity (Figure S3B). What's more, we could also find that 8 chemical or targeted drugs, which applied to LUAD therapy, showed lower IC50 in the low-risk group (Figure S4).

Changes of cell proliferation level after transfection of siRNAs

In order to explore the effect of NRIncRNAs on the proliferation of tumor cells in vitro, we transfected siRNAs targeting NRIncRNAs in A549 cell line, respectively. Our data showed that all lncRNAs were successfully knocked down (**Figure 7**). The A549 cell colony formation assays indicated that the LUAD cell proliferation capacity was decreased significantly after LINC01281, AL606489.1, AL157823.2, MED-AS1, FAM83A-AS1 knockdown. However, after the expression of LINC01290 and AL031600.2 decreased, the proliferation ability of cells increased to some extent (**Figure 8A**).

Changes of PD1 and CD28 level after transfection with siRNA

PD1 and CD28 are immune checkpoints commonly used in scientific research and clinical work [22, 23]. Recent publications on PD1 have highlighted a new signaling paradigm of PD1 for tumor regulation. Moreover, CD28 is also widely expressed on the lymphocytes and has been reported to regulate tumor progression [24]. Therefore, we used PCR to detect the expression levels of PD1 and CD28 after transfection with siRNAs. The decrease of expression level of PD1 was accompanied by the decrease of LINC01281, MED4-AS1, and FAM83A-AS1 level, while increased with the downregulation of AL031600.2, LINC01290, AC026355.2 (**Figure 8B**). As is shown in (**Figure 8C**), the level of LINC01281, AL157823.2 and FAM83A-AS1 were negatively correlated with the level of CD28.

Discussion

With the increasing development of computer technology and artificial intelligence in the field of medical biology, bioinformatics has become one of the necessary tools for exploring diverse diseases on the basis of public datasets, such as TCGA and Gene Expression [25-29]. Over the past few years, the risk signatures based on bioinformatics analysis for predicting the prognosis of patients with cancers have become more and more popular [19, 30, 31]. Although there were several signatures utilizing NRGs or NRIncRNAs to forecast the prognosis of cancers patients, such as colon cancer, gastric cancer and pancreatic adenocarcinoma [21, 31, 32], the present study is the first to explore the NRIncRNA model in detail. We conducted a detailed study on the tumor immunity of the NRIncRNA signature, which renders the constructed signature applicable for guiding the clinical personalized treatment of patients with LUAD.

In this study, first, NRGs were obtained through published literatures, and 20 NRIncRNAs with prognostic value were screened on the basis of co-expression analysis and univariate Cox analysis. Nine key NRIncRNAs (*AL031600.2, LINC01281, AP001178.1, AL157823.2, LINC01290, MED4-AS1, AC026355.2, AL606489.1, FAM83A-AS1*) were filtered out to construct the prognostic signature of LUAD using LASSO regression analysis. The survival analysis and risk score distribution of 9 NRIncRNAs indicated that patients with up-regulated AP001178.1, AL157823.2, AL606489.1, FAM83A-AS1 and down-regulated AL031600.2, LINC01281, LINC01290, MED4-AS1, AC026355.2 had higher risk scores and were more likely to have poor prognosis ($P < 0.05$). Next, the 1-, 2- and 3-year AUC showed that the model had good sensitivity and specificity in predicting the prognosis of LUAD. We also carried out univariate and multivariate Cox regression analysis on risk score and other clinical predictors, which proved that risk score could be used as an independent prognostic factor for LUAD patients. TNM stage is an internationally recognized predictor of clinical outcomes. Correlation analysis between risk score and clinicopathologic features showed that risk score was closely related to age, gender, T stage, N stage, tumor stage and poor prognosis, but the causal relationship between them still needs further exploration.

At present, there are many studies on FAM83A-AS1 in the nine NRIncRNAs finally included in

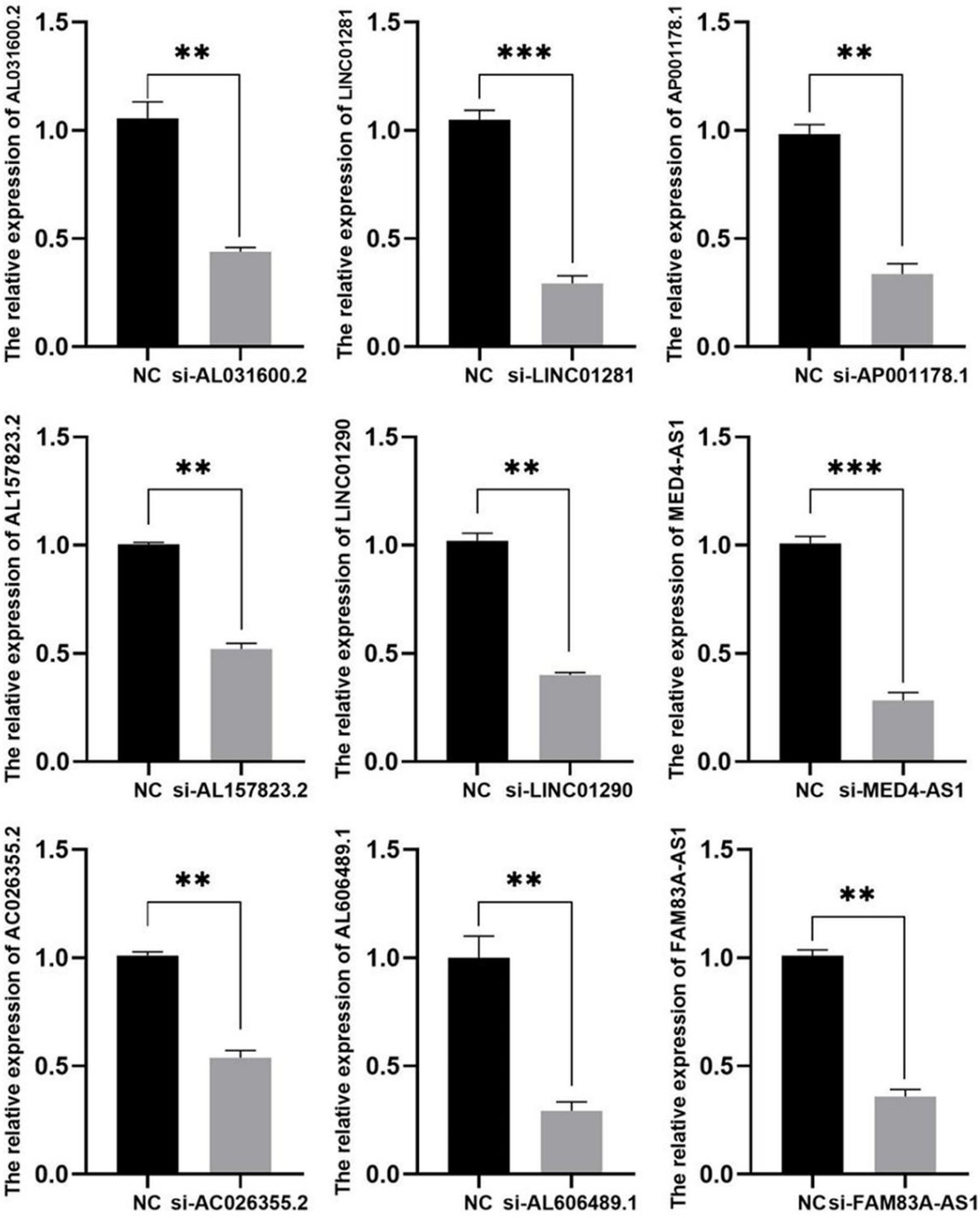

Figure 7. NRIncRNAs knock-down efficiency verification. qRT-PCR assay. The results showed that the expression levels of NRIncRNAs decreased significantly with the transfection of siRNAs. ***P < 0.01* and ****P < 0.001.*

the model. Many studies have confirmed that FAM83A-AS1 has biological behaviors such as promoting tumor growth and proliferation in a variety of tumors, including liver cancer, esophageal squamous cell carcinoma and lung cancer [33-35]. FAM83A-AS1 is up-regulated in lung adenocarcinoma tissues, and its high expression is closely related to low OS and progression-free survival in LUAD patients, which is consistent with our results [36]. Knockout of

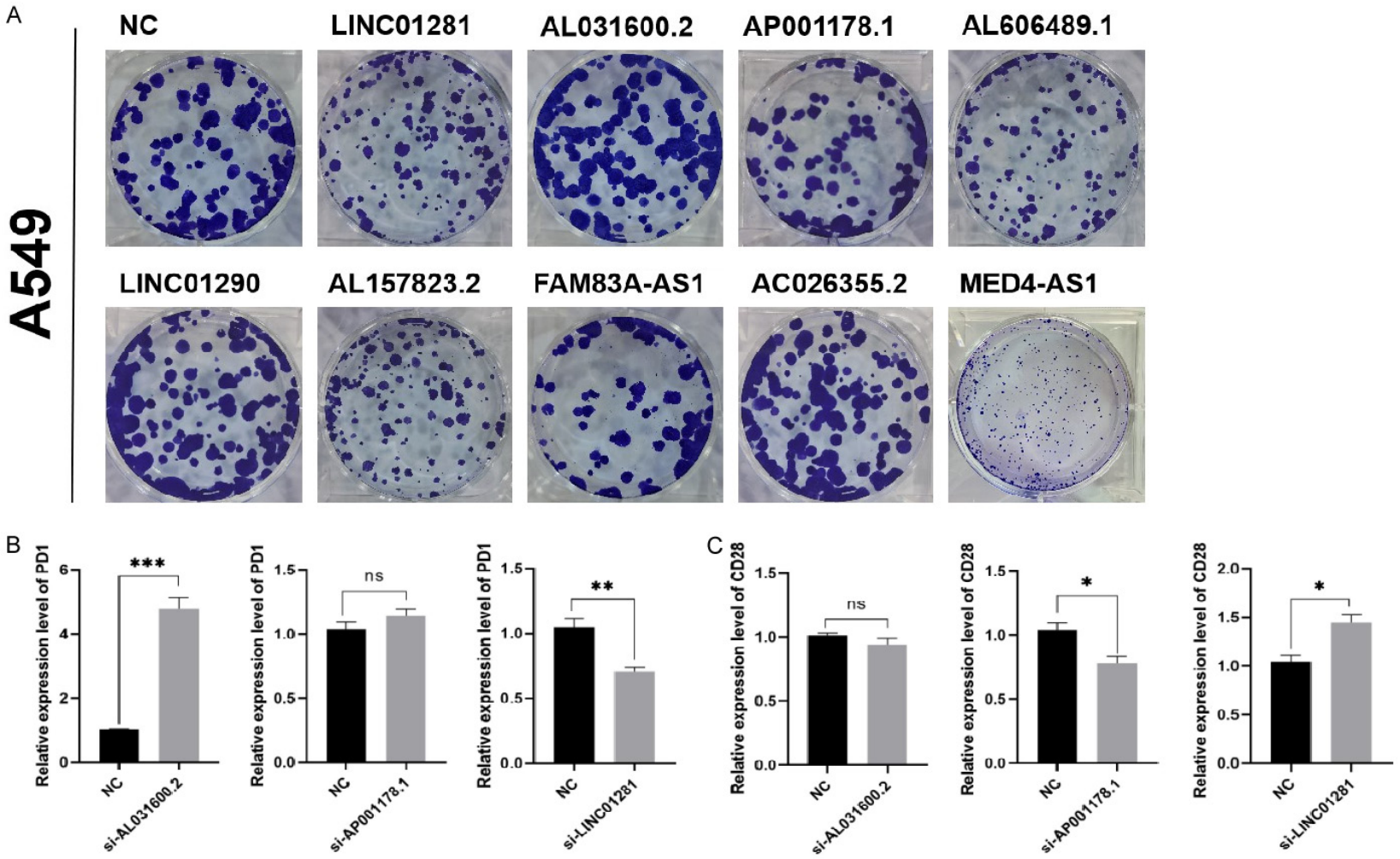
A
A549
NC
LINC01281
AL031600.2
AP001178.1
AL606489.1
LINC01290
AL157823.2
FAM83A-AS1
AC026355.2
MED4-AS1
B
Relative expression level of PD1
***
ns
**
NC
si-AL031600.2
si-AP001178.1
si-LINC01281
C
Relative expression level of CD28
ns
*
*

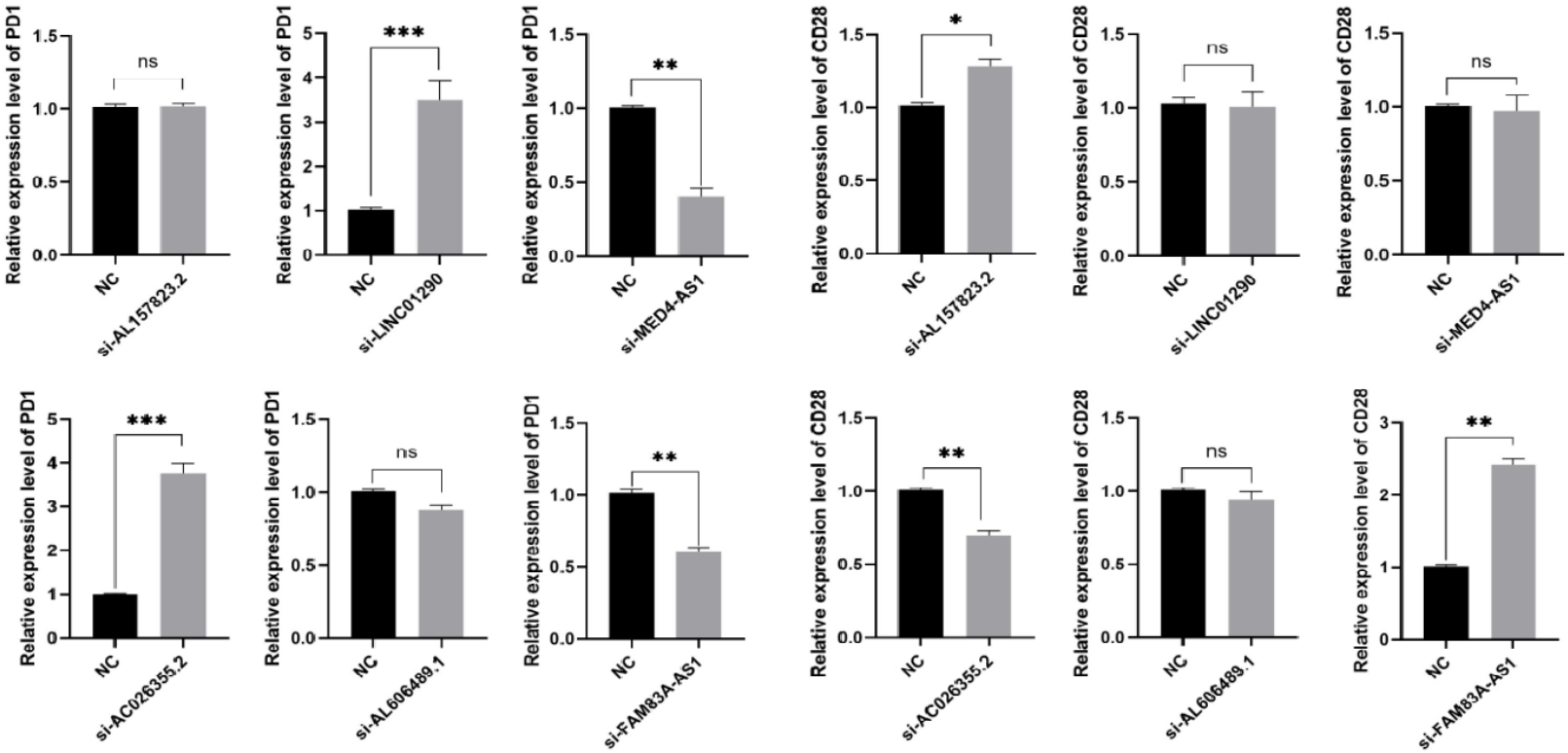

Figure 8. Verification of cell proliferation capicity and immune checkpoints expression levels. A. Colony formation assay. The assay indicated that Linc01281, AL606489.1, AL157823.2, MED-AS1 and FAM83A-AS1 are positively correlated with the proliferation level of LUAD cells. While LINC01290 and AL031600.2 are involved in the negative regulation of LUAD cell proliferation. B. qRT-PCR assay. The data confirmed that LINC01281, MED4-AS1, and FAM83A-AS1 significantly inhibited the expression of PD1, whereas AL031600.2, LINC01290, AC026355.2 promoted the expression of PD1. C. qRT-PCR assay. The data displayed the increased expression level of CD28 when LINC01281, AL157823.2 and FAM83A-AS1 reduced. *$P < 0.05$ and **$P < 0.01$.

FAM83A-AS1 could inhibit the proliferation, migration and invasion of LUAD cells [37, 38]. The experiment confirmed that FAM83A-AS1 promoted lung cancer progression by ERK and HIF-1α/glycolysis signaling pathways. Tang et al. found that MED4-AS1 existed in the nucleus and cytoplasm of A549 cells, which was significantly correlated with women, low differentiation and lymph node metastasis ($P < 0.05$). It can be seen that although there are many studies on lncRNAs related to the prognosis of lung adenocarcinoma, there are few studies on 11 lncRNAs included in the prognosis lncRNA model of lung adenocarcinoma.

In summary, we developed a novel signature involving 9 NRlncRNAs (*AL031600.2, LINC01281, AP001178.1, AL157823.2, LINC01290, MED4-AS1, AC026355.2, AL606489.1, FAM83A-AS1*) that can accurately predict the outcome of LUAD and are associated with the immune response. This will provide new insights into the development of new therapies for LUAD. The risk model based on the 9 NRlncRNAs can well separate the patients with lung adenocarcinoma into high- and low-risk groups, which provides a certain basis for the prognosis prediction of patients with lung adenocarcinoma and the formulation of individualized treatment plans.

Acknowledgements

This study was funded by National Natural Science Foundation of China (No. 82070096).

Disclosure of conflict of interest

None.

Address correspondence to: Dr. Yanwei Chen, Department of Pulmonary Critical Care Medicine, The Second Affiliated Hospital of The Air Force Military Medical University, Xinsi Road 569, Xi'an 710038, Shaanxi, PR China. E-mail: chenyw@szu.edu.cn

References

[1] Siegel RL, Miller KD, Fuchs HE and Jemal A. Cancer statistics, 2022. CA Cancer J Clin 2022; 72: 7-33.

[2] Lortet-Tieulent J, Soerjomataram I, Ferlay J, Rutherford M, Weiderpass E and Bray F. International trends in lung cancer incidence by histological subtype: adenocarcinoma stabilizing in men but still increasing in women. Lung Cancer 2014; 84: 13-22.

[3] Wang M, Herbst RS and Boshoff C. Toward personalized treatment approaches for non-small-cell lung cancer. Nat Med 2021; 27: 1345-1356.

[4] Herbst RS, Morgensztern D and Boshoff C. The biology and management of non-small cell lung cancer. Nature 2018; 553: 446-454.

[5] Johnstone RW, Ruefli AA and Lowe SW. Apoptosis: a link between cancer genetics and chemotherapy. Cell 2002; 108: 153-164.

[6] Gong Y, Fan Z, Luo G, Yang C, Huang Q, Fan K, Cheng H, Jin K, Ni Q, Yu X and Liu C. The role of necroptosis in cancer biology and therapy. Mol Cancer 2019; 18: 100.

[7] Strilic B, Yang L, Albarran-Juarez J, Wachsmuth L, Han K, Muller UC, Pasparakis M and Offermanns S. Tumour-cell-induced endothelial cell necroptosis via death receptor 6 promotes metastasis. Nature 2016; 536: 215-218.

[8] Yang L, Joseph S, Sun T, Hoffmann J, Thevissen S, Offermanns S and Strilic B. TAK1 regulates endothelial cell necroptosis and tumor metastasis. Cell Death Differ 2019; 26: 1987-1997.

[9] Yan J, Wan P, Choksi S and Liu ZG. Necroptosis and tumor progression. Trends Cancer 2022; 8: 21-27.

[10] Jaime-Sanchez P, Catalan E, Uranga-Murillo I, Aguilo N, Santiago L, M Lanuza P, de Miguel D, A Arias M and Pardo J. Antigen-specific primed cytotoxic T cells eliminate tumour cells in vivo and prevent tumour development, regardless of the presence of anti-apoptotic mutations conferring drug resistance. Cell Death Differ 2018; 25: 1536-1548.

[11] Seifert L, Werba G, Tiwari S, Ly NNG, Alothman S, Alqunaibit D, Avanzi A, Barilla R, Daley D, Greco SH, Torres-Hernandez A, Pergamo M, Ochi A, Zambirinis CP, Pansari M, Rendon M, Tippens D, Hundeyin M, Mani VR, Hajdu C, Engle D and Miller G. Author correction: the necrosome promotes pancreatic oncogenesis via CXCL1 and Mincle-induced immune suppression. Nature 2021; 591: E28.

[12] Liu W, Jin W, Zhu S, Chen Y and Liu B. Targeting regulated cell death (RCD) with small-molecule compounds in cancer therapy: a revisited review of apoptosis, autophagy-dependent cell death and necroptosis. Drug Discov Today 2022; 27: 612-625.

[13] Grixti JM and Ayers D. Long noncoding RNAs and their link to cancer. Noncoding RNA Res 2020; 5: 77-82.

[14] Bhan A and Mandal SS. Long noncoding RNAs: emerging stars in gene regulation, epigenetics and human disease. ChemMedChem 2014; 9: 1932-1956.

[15] Chi Y, Wang D, Wang J, Yu W and Yang J. Long non-coding RNA in the pathogenesis of cancers. Cells 2019; 8: 1015.
[16] He J, Zhu S, Liang X, Zhang Q, Luo X, Liu C and Song L. LncRNA as a multifunctional regulator in cancer multi-drug resistance. Mol Biol Rep 2021; 48: 1-15.
[17] Jiang N, Meng X, Mi H, Chi Y, Li S, Jin Z, Tian H, He J, Shen W, Tian H, Pan J, Fang S, Jin X, Zhou C and Gong Z. Circulating lncRNA XLOC_009167 serves as a diagnostic biomarker to predict lung cancer. Clin Chim Acta 2018; 486: 26-33.
[18] Yue T, Chen S, Zhu J, Guo S, Huang Z, Wang P, Zuo S and Liu Y. The aging-related risk signature in colorectal cancer. Aging (Albany NY) 2021; 13: 7330-7349.
[19] Yang X, Weng X, Yang Y, Zhang M, Xiu Y, Peng W, Liao X, Xu M, Sun Y and Liu X. A combined hypoxia and immune gene signature for predicting survival and risk stratification in triple-negative breast cancer. Aging (Albany NY) 2021; 13: 19486-19509.
[20] Song Q, Shang J, Yang Z, Zhang L, Zhang C, Chen J and Wu X. Identification of an immune signature predicting prognosis risk of patients in lung adenocarcinoma. J Transl Med 2019; 17: 70.
[21] Wang N and Liu D. Identification and validation a necroptosis-related prognostic signature and associated regulatory axis in stomach adenocarcinoma. Onco Targets Ther 2021; 14: 5373-5383.
[22] Ohaegbulam KC, Assal A, Lazar-Molnar E, Yao Y and Zang X. Human cancer immunotherapy with antibodies to the PD-1 and PD-L1 pathway. Trends Mol Med 2015; 21: 24-33.
[23] Zhang Q, Tang L, Zhou Y, He W and Li W. Immune checkpoint inhibitor-associated pneumonitis in non-small cell lung cancer: current understanding in characteristics, diagnosis, and management. Front Immunol 2021; 12: 663986.
[24] Huff WX, Kwon JH, Henriquez M, Fetcko K and Dey M. The evolving role of CD8(+)CD28(-) immunosenescent T cells in cancer immunology. Int J Mol Sci 2019; 20: 2810.
[25] Gauthier J, Vincent AT, Charette SJ and Derome N. A brief history of bioinformatics. Brief Bioinform 2019; 20: 1981-1996.
[26] Canzoneri R, Lacunza E and Abba MC. Genomics and bioinformatics as pillars of precision medicine in oncology. Medicina (B Aires) 2019; 79: 587-592.
[27] Wang X, Williams C, Liu ZH and Croghan J. Big data management challenges in health research-a literature review. Brief Bioinform 2019; 20: 156-167.
[28] Schlick CJR, Castle JP and Bentrem DJ. Utilizing big data in cancer care. Surg Oncol Clin N Am 2018; 27: 641-652.
[29] Chen L, Li H, Xie L, Zuo Z, Tian L, Liu C and Guo X. Editorial: big data and machine learning in cancer genomics. Front Genet 2021; 12: 749584.
[30] Gao X, Tang M, Tian S, Li J and Liu W. A ferroptosis-related gene signature predicts overall survival in patients with lung adenocarcinoma. Future Oncol 2021; 17: 1533-1544.
[31] Huang Y, Zou Y, Xiong Q, Zhang C, Sayagues JM, Shelat VG and Wang X. Development of a novel necroptosis-associated miRNA risk signature to evaluate the prognosis of colon cancer patients. Ann Transl Med 2021; 9: 1800.
[32] Wu Z, Huang X, Cai M, Huang P and Guan Z. Novel necroptosis-related gene signature for predicting the prognosis of pancreatic adenocarcinoma. Aging (Albany NY) 2022; 14: 869-891.
[33] Huang GM, Zang HL, Geng YX and Li YH. LncRNA FAM83A-AS1 aggravates the malignant development of esophageal cancer by binding to miR-495-3p. Eur Rev Med Pharmacol Sci 2020; 24: 9408-9415.
[34] Shen S, Wu Y, Chen J, Xie Z, Huang K, Wang G, Yang Y, Ni W, Chen Z, Shi P, Ma Y and Fan S. CircSERPINE2 protects against osteoarthritis by targeting miR-1271 and ETS-related gene. Ann Rheum Dis 2019; 78: 826-836.
[35] He J and Yu J. Long noncoding RNA FAM83A-AS1 facilitates hepatocellular carcinoma progression by binding with NOP58 to enhance the mRNA stability of FAM83A. Biosci Rep 2019; 39: BSR20192550.
[36] Wang W, Zhao Z, Xu C, Li C, Ding C, Chen J, Chen T and Zhao J. LncRNA FAM83A-AS1 promotes lung adenocarcinoma progression by enhancing the pre-mRNA stability of FAM83A. Thorac Cancer 2021; 12: 1495-1502.
[37] Chen Z, Hu Z, Sui Q, Huang Y, Zhao M, Li M, Liang J, Lu T, Zhan C, Lin Z, Sun F, Wang Q and Tan L. LncRNA FAM83A-AS1 facilitates tumor proliferation and the migration via the HIF-1alpha/glycolysis axis in lung adenocarcinoma. Int J Biol Sci 2022; 18: 522-535.
[38] Wang G, Li X, Yao Y, Jiang Z, Zhou H, Xie K, Luo J and Shen Y. FAM83A and FAM83A-AS1 both play oncogenic roles in lung adenocarcinoma. Oncol Lett 2021; 21: 297.

Table S1. 67 necroptosis-related genes

Genes			
FADD	PLK1	MAP3K7	TNFRSF21
FAS	MPG	SQSTM1	OTULIN
FASLG	BACH2	STAT3	CYLD
MLKL	GATA3	DIABLO	USP22
RIPK1	MYCN	DNMT1	TARDBP
RIPK3	ALK	CFLAR	APP
TLR3	ATRX	BRAF	BNIP3
TNF	TERT	AXL	CD40
TSC1	SLC39A7	ID1	BCL2L11
TRIM11	SPATA2	CDKN2A	EGFR
CASP8	RNF31	HSPA4	DDX58
ZBP1	IDH1	BCL2	TNFRSF1A
MAPK8	IDH2	STUB1	TNFSF10
IPMK	KLF9	FLT3	TNFRSF1B
ITPK1	HDAC9	HAT1	TRAF2
SIRT3	HSP90AA1	SIRT2	PANX1
MYC	LEF1	SIRT1	

Table S2. 20 necroptosis-related lncRNAs screened by Univrariant Cox regression analysis

id	HR	HR.95L	HR.95H	*p* value
TBX5-AS1	0.664688196	0.452609985	0.976139308	0.037238915
AL031600.2	0.174703569	0.035143244	0.868483761	0.032982224
AC091057.1	1.849136917	1.017079866	3.361886761	0.043853205
AC005884.1	0.347863946	0.126262253	0.958396687	0.041137212
PTPRN2-AS1	0.391752988	0.20010532	0.766948142	0.00625527
AC018647.1	0.097712027	0.010571775	0.903125547	0.040387141
LINC01281	0.273402342	0.087211643	0.857097028	0.026116354
AP001178.1	3.050599444	1.168893655	7.961508666	0.022678068
AL157823.2	2.108132373	1.008952006	4.404790389	0.04729282
AC007671.1	0.141582489	0.031666918	0.633013966	0.01051561
LINC01290	0.414341472	0.198294099	0.865778944	0.019114995
AC103591.3	0.654292863	0.439021656	0.975120805	0.037185705
AP000695.1	1.699267518	1.125677053	2.565131881	0.011622639
MED4-AS1	0.337591582	0.126519111	0.90079732	0.03011285
AC026355.2	0.617271532	0.438609738	0.868708812	0.005652589
AL606489.1	1.832957705	1.318668771	2.547822486	0.000310526
AC110619.1	1.375441381	1.006096694	1.88037492	0.045709971
AC099850.3	1.248153428	1.02204709	1.524281019	0.029718172
TMPO-AS1	1.660391694	1.049595241	2.626632127	0.030249082
FAM83A-AS1	1.391722252	1.145227431	1.691271773	0.000889421

Table S3. All primers used for qPCR analysis

Gene	Primers sequences
GAPDH	5'-CAGGAGGCATTGCTGATGAT-3'
	5'-GAAGGCTGGGGCTCATTT-3'
AL031600.2	5'-CCGGCCAGAATGATCCGTTA-3'
	5'-GCACTTCTCTCTAACGCCACT-3'
LINC01281	5'-GCTGTGCCAATGCTCACAAA-3'
	5'-AGCCTCCCAATACTCACATGG-3'
AC026355.2	5'-GGATGATGATGGACAGATGCCT-3'
	5'-GTGGACAGGGACCATTGTGA-3'
AL157823.2	5'-CCCATCGCATCTCCACTGAA-3'
	5'-AGTGGTTCCAGATTTCTGTGCT-3'
AP001178.1	5'-ACCAGCTAAATCACATCTCAAGAC-3'
	5'-GCCAAGATACTCAAGGAAGGC-3'
LINC01290	5'-AAAATGATGAACGCACGACGG-3'
	5'-AGAGCCCAACATCCTTGCTG-3'
MED4-AS1	5'-TGTGGAGCAAGGACATCTGG-3'
	5'-TGCCAGGTAATGTTAAGCCGA-3'
AL606489.1	5'-GGAAATAGACCACTCCTGCCT-3'
	5'-TGGGACTGAAAGGGCAAAGT-3'
FAM83A-AS1	5'-AGGCCCAACTCCAGCCAA-3'
	5'-TTCAACACTGAAGGGCTGGTT-3'

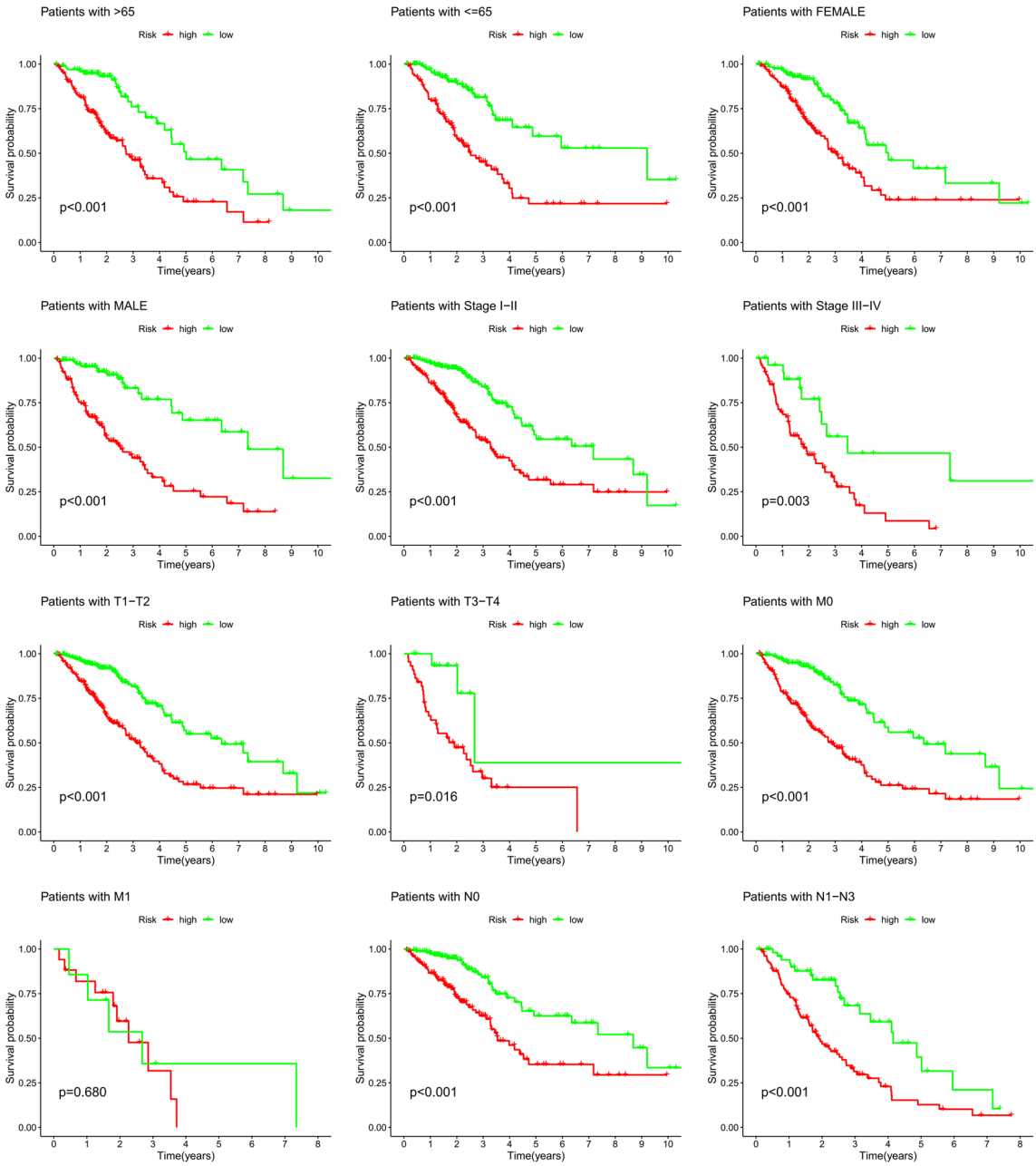

Figure S1. Kaplan-Meier survival curves of OS (survival probability) prognostic value stratified by age, gender, grade, stage, T, N, or M between low- and high-risk groups in the entire set.

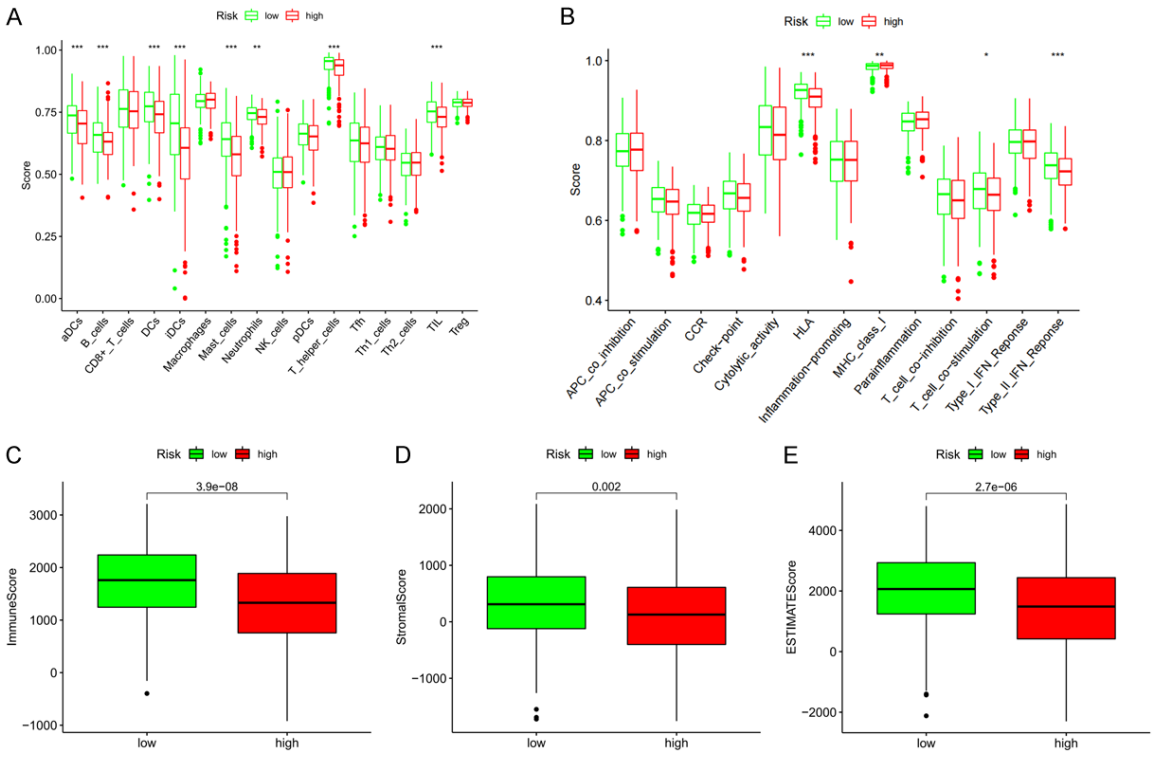

Figure S2. ssGSEA analysis. (A) Comparison of the enrichment scores of 16 types of immune cells and (B) 13 immune-related pathways between low- (green box) and high-risk (red box) group in the TCGA cohort. (C-E) The comparison of immune-related scores between low- and high-risk groups, which showed low-risk group exhibited much higher immune score, stromal score and ESTIMATE score. **P < 0.05*, ***P < 0.01 and ***P < 0.001.*

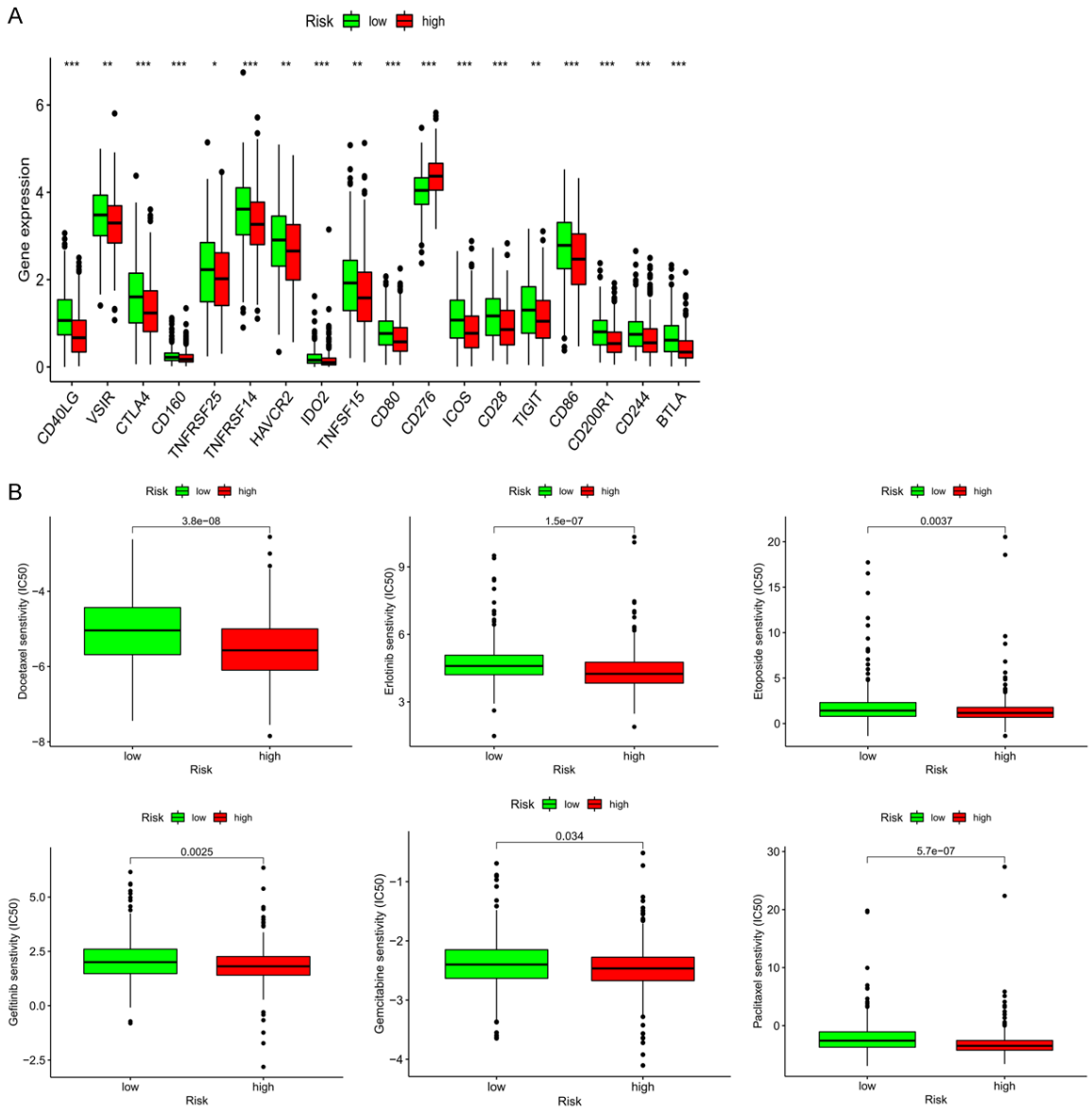

Figure S3. Investigation of the TME and Immune Checkpoints. A. The expression of 18 checkpoints in risk groups, which showed only CD276 was highly expressed in high-risk patients. B. Differences in the response to targeted therapy between high-risk and low-risk groups. Patients with low-risk scores were highly sensitive to the targeted therapeutics gefitinib and erlotinib. In addition, patients with low-risk scores were highly sensitive to the chemotherapeutics etoposide, paclitaxel, docetaxel and Gemcitabine. *$P < 0.05$, **$P < 0.01$ and ***$P < 0.001$.

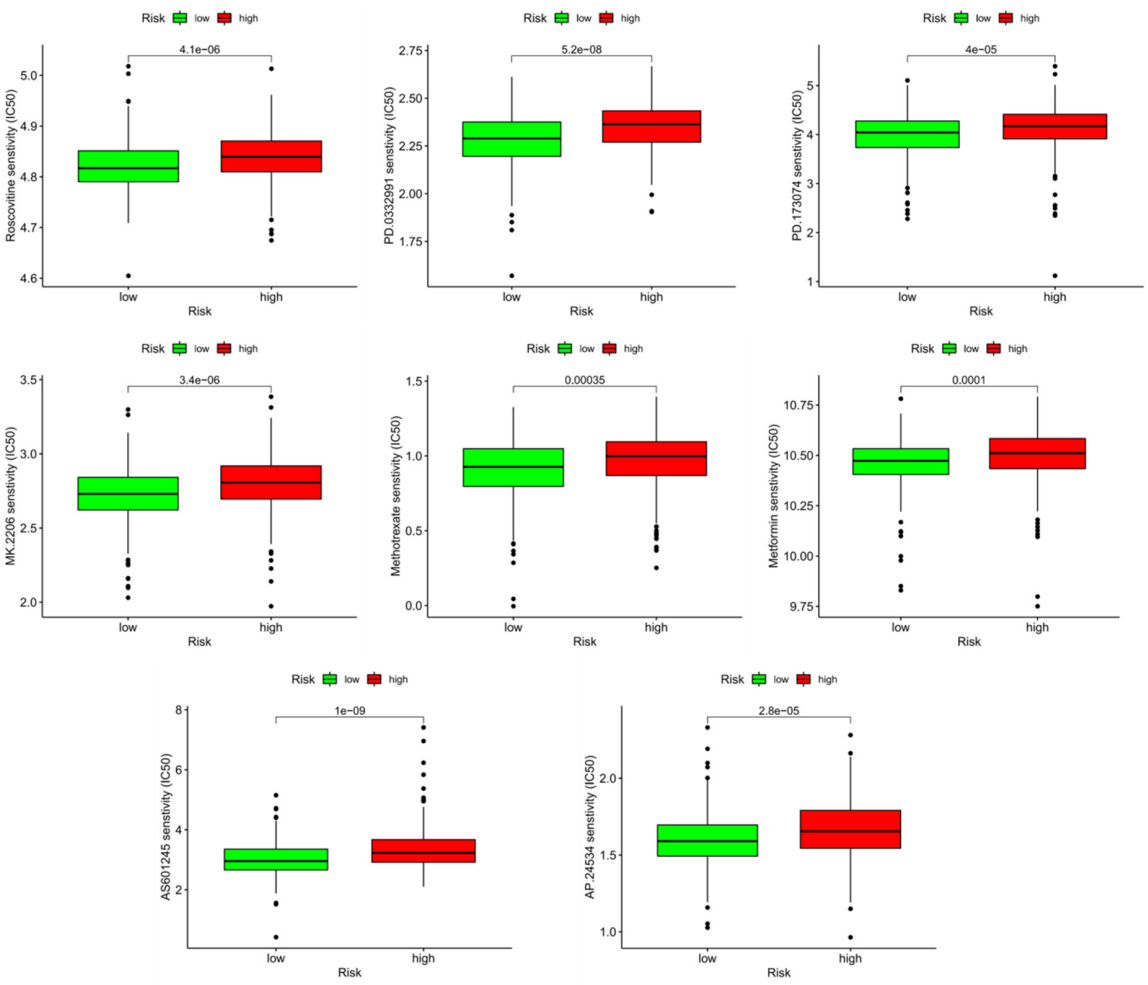

Figure S4. The immunotherapy prediction of risk groups, including PD.173074, AP.24534, Metformin, Methotrexate, Roscovitine, MK.2206, PD.0332991 and AS601245.